The DLR CO_2-equivalent estimator FlightClim v1.0: an easy-to-use estimation of per flight CO_2 and non-CO_2 climate effects

Hannes Bruder[1], Robin N. Thor[2], Malte Niklaß[1], Katrin Dahlmann[2], Roland Eichinger[2], Florian Linke[1], Volker Grewe[2, 3], Sigrun Matthes[2], and Simon Unterstrasser[2]

[1]Deutsches Zentrum für Luft- und Raumfahrt (DLR), Institut für Luftverkehr, Hamburg, Germany
[2]Deutsches Zentrum für Luft- und Raumfahrt (DLR), Institut für Physik der Atmosphäre, Oberpfaffenhofen, Germany
[3]Faculty of Aerospace Engineering, Operations and Environment, Delft University of Technology, Delft, The Netherlands

Correspondence: Hannes Bruder (hannes.bruder@dlr.de)

Abstract. As aviation's contribution to anthropogenic climate change is increasing, the sector aims at reducing its climate effect in accordance with international agreements. The strong and variable non-CO_2 effects are complex, making reliable climate effect quantification a necessary first step. To support this, we develop the easy-to-use first-order climate effect estimator for single flights *FlightClim v1.0*. The tool estimates the flight-specific climate effect with a simplified calculation model, without requiring detailed information on exact routing, amount of fuel burn, or weather conditions.

For this purpose, we first analyze a global flight dataset containing detailed trajectories, associated flight emissions, and climate responses. Similar flights are grouped into clusters, and regression formulas are derived to estimate the Average Temperature Response over 100 years (ATR100) for CO_2 and non-CO_2 effects. To prevent abrupt changes at cluster boundaries, we apply linear smoothing as postprocessing. Second, we compare a Multiple and a Symbolic Regression approach, where choice of method depends on the specific application as they differ in effort and complexity. The two approaches offer similar estimation quality, which shows that the errors are based on the database, the regression parameters as well as the regression error metric and the physical processes rather than on too easy regression models. Both methods are designed for climate footprint assessments due to their simplicity though not suitable for policy measures. Emission trading or monitoring and reporting systems instead require detailed weather and route data to incentivize operational non-CO_2 mitigation. Compared to previous studies, our approach relies on a globally representative and considerably larger dataset covering more aircraft types, including most commercial airliners. In addition it improves precision through smoothed clustering and a dedicated parameterization of aircraft size influence on the contrail effects.

The resulting climate effect functions are embedded into the Excel-based tool *FlightClim v1.0*, which implements the formulas of the Multiple Regression approach due to slight qualitative advantages. Requiring only aircraft size and origin-destination airports as input, *FlightClim* estimates climate effect for CO_2, H_2O, NO_x emissions and contrail-induced cloudiness. It includes per seat allocation and supports different climate metrics.

1 Introduction

Global aviation more than doubled from 2006 to 2019 in terms of revenue passenger kilometers (ICAO, 2015, 2021). The associated CO_2 emissions grew by 40% to 1036 $\mathrm{Tg(CO_2)yr^{-1}}$ during this time span (IEA, 2022). After the considerable reduction of air transportation through COVID-19, it reached pre-pandemic levels again by 2023 and now continues to grow (Economics, 2024). Projections show that aviation's share in global CO_2 emissions could rise from currently about 2% to 22% in 2050 (Cames et al., 2015). This amplifies the pressure on the sector for finding solutions to reach the Paris agreement climate goals.

A number of measures are suited to reduce the climate effect of aviation ranging from technological (i.a. Dahlmann et al., 2016b; Silberhorn et al., 2022; Delbecq et al., 2023) and fuel-related solutions (e.g. Teoh et al., 2022; Märkl et al., 2024; Quante et al., 2025) to operational (i.a. Grewe et al., 2014, 2017b; Lührs et al., 2016, 2021; Teoh et al., 2020; Matthes et al., 2021; Yin et al., 2023; Martin Frias et al., 2024; Sausen et al., 2024) and regulatory options (i.a. Scheelhaase et al., 2016; Larsson et al., 2019; Niklaß et al., 2021, 2025). To be overall effective, these measures do not only need to target the reduction of CO_2 emissions, but also the so called non-CO_2 effects. Non-CO_2 effects were responsible for about two thirds of the total effective radiative forcing (ERF) in 2018 when considering all aviation emissions from 1940 to 2018 (Lee et al., 2021). Especially the effects of persistent contrail cirrus formation and of NO_x emissions on the ozone concentration increase the total impact of air traffic on the climate. The uncertainties of the non-CO_2-effects are high compared to the climate effect of CO_2 emissions, according to Lee et al. (2021) about 60 % for H_2O emissions, 65 % to 95 % for NO_x emissions and 70 % for contrail-induced cloudiness (CiC).

The basis for the development of effective mitigation measures, as well as the first step for climate effect compensation programs is a reliable estimate of the total climate effect of a flight, including the non-CO_2 effects. However, while the CO_2 climate effect can be estimated easily, as it is independent of emission source, location and time, the effects of non-CO_2 emissions are much more complex to determine (Dahlmann et al., 2023). For simplicity, often the global ratio of non-CO_2 to CO_2 climate effects is used as a factor for total climate effect estimation, based solely on CO_2 emissions. An example of this simple estimation option for aviation is the Radiative Forcing Index (RFI, IPCC, 1999), which is the ratio of the total radiative forcing to the radiative forcing of CO_2 emissions.

However, Forster et al. (2006) highlighted the limiting shortcomings of the RFI concept, such as a large variation with time for constant emissions, and concluded that RFI is inappropriate for comparing emissions. In addition, the altitude dependency of non-CO_2 effects has to be considered in the estimation method to avoid misguiding incentives (Faber et al., 2008; Scheelhaase et al., 2016; Niklaß et al., 2019). However, this requires detailed information of the flown trajectory, the aircraft and atmospheric conditions to estimate the various climate effects. To query this data is an elaborate process, public accessibility is limited and the data is not available before the flight. Hence, a simplified estimation method that is easy to use for the climate footprint assessment of single flights yet realistically representing non-CO_2 climate effects is needed.

There are a few methods for simplified climate footprint assessment of single flights publicly available. Popular ones are the "ICAO Carbon Emissions Calculator" (ICAO, 2025), the "Flight Emissions Label" of the European Union (EASA, 2025),

the "Aviation 1 Master emissions calculator 2023" of the European Environment Agency (EEA, 2023), Google´s "Travel Impact Module" (Google, 2025) and the "myclimate flight emission calculator" (Foundation myclimate, 2025). All of them have particular areas of application and strengths, but all of them only take into account CO_2-emissions, use constant factors to quantify non-CO_2-effects or are lacking the climate effect of CiC. A method that overcomes these shortcomings and only relies on mission parameters as distance and geographic flight region has been introduced by Dahlmann et al. (2023). Dahlmann et al. (2023) analyzed the climate effect of the typical long-haul aircraft type Airbus A330-200 for more than 1000 international city pairs using the climate response model AirClim (Grewe and Stenke, 2008; Dahlmann et al., 2016a) and then fitted altitude and latitude dependent regression formulas to the AirClim results. The regression formulas enable an easy to use estimation of the ratio of H_2O, NO_x and CiC climate effect in relation to the CO_2 climate effect of single flights and show a much better estimation quality than a constant factor. While the root mean square error for a constant factor of 3.4 for the ratio of total climate effect to the one of CO_2 was about 1.18 [-], the one obtained with the regression formulas was about 0.24 [-], with 95% of the estimates lying within a $\pm 20\%$ range for the A330-dataset. However, there is no easy-to-use method available that provides a thorough estimate of the non-CO_2 climate effects for individual passengers or organizations, allowing them to assess their footprint pre-flight for travel decisions and post-flight to track their personal climate impact, without requiring detailed information about the actual flown trajectory, the amount of emissions produced and the prevailing weather situation. Such a method would also enables a quick climate effect estimation for large flightplans, supporting scientific research and organizational carbon accounting.

In the present study, we expand the work by Dahlmann et al. (2023) and develop an easy-to-use estimation method for aircraft climate effects, using climate effect regression functions that are valid for all jet passenger aircraft with a seat capacity of over 20. While Dahlmann et al. (2023) only analyzed one aircraft type, we here analyze the climate effect for various commercial aircraft. Instead of using constant emissions over a typical aircraft lifetime of 32 years, we here use the more realistic assumption of increasing emissions over the next 100 years, which influences the weighting of the individual non-CO_2 effects according to Megill et al. (2024). We consider the climate effects of aircraft emissions of CO_2, NO_x, and H_2O as well as CiC, but exclude the effects of aerosol emissions through aerosol–radiation interactions and aerosol–cloud interactions as the understanding and assessment is not yet mature enough to be included here. This easy-to-use method is only based on the aircraft size as well as the distance and latitude of the flight, and the two latter quantities can be easily computed from the airport pair.

The method is based on the combination of atmospheric climate response surfaces, that are derived from chemistry-climate model simulations, and a detailed 3-D aviation emission inventory for a full year. From those AirClim estimates the individual flights‘ climate response that serves as the regression database. The derived *FlightClim* regression models are route and aircraft specific parametrisations of the flight-specific climate effects. The described modeling workflow is depicted in Figure 1.

The paper is structured as follows. In the first step, we describe the preparation of the regression flight dataset including a distance and latitude dependent clustering (Section 2). Then we apply both Multiple Regression (MR) and Symbolic Regression (SR) to generate specific climate effect regression functions for each cluster (Section 3). Finally, we compare and discuss the

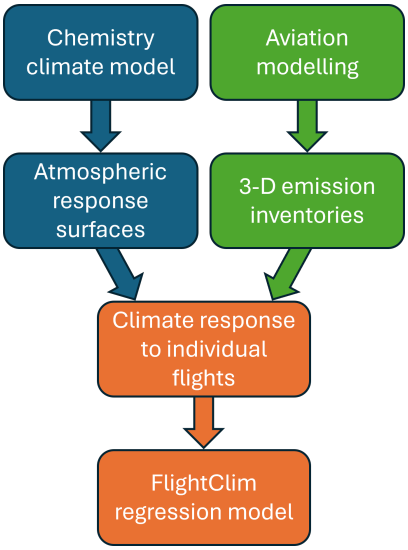

Figure 1. High–level modelling workfow *FlightClim* is based on.

resulting formulas for the climate effect of individual flights (Section 3.4). The resulting equations have been implemented into an easy-to-use estimation tool, for which the user manual is available in Section S7 of the Supplementary Material.

We want to stress here that the method presented in this paper, is not intended to assess the effects of neither individual trajectories, weather situations, specific aircraft or different aircraft generations/technologies.

2 Preparation of the regression dataset

The regression formulas for the estimation of the climate effect of single flights are based on a dataset consisting of about 57 thousand flight trajectory simulations. These simulations represent global jet-powered civil aviation, covering approximately 30 million flights on 21 thousand routes between 11 thousand city pairs, which accounts for 98% of globally available seat kilometers (ASK). The dataset is derived from a global flightplan of the year 2012, which serves as the base for the creation of flight emission inventories (Section 2.1). The inventories are then used to derive the climate effect per flight, that represents the dependent variable of the regression (Section 2.2). In the final step of the dataset preparation a clustering is derived to group similar flights for the regression analysis (Section 2.3).

2.1 Global emission inventory

As the basis for the derivation of regression formulas for climate effect estimation, data from the project WeCare (Utilizing WEather information for ClimAte efficient and ecoefficient futuRE aviation, Grewe et al., 2017a) was used, which was an internal project of the German Aerospace Center (Deutsches Zentrum für Luft- und Raumfahrt; DLR). The project addressed both an improvement of the understanding of aviation-influenced atmospheric processes and an assessment of different mitigation

options. An essential output of the project was a new set of emission inventories for global aviation (Grewe et al., 2017a). The network of flight trajectories was developed following a four-layer approach implemented in the AIRCAST method (Ghosh et al., 2016). It is starting from an origin–destination passenger demand network that was built up from exogenous socio-economic scenarios, via the passenger routes network (sequence of flight segments, a passenger actually travelled from origin to destination) to an aircraft movements network, which assigns aircraft seat categories to the resulting flight routes and provides flight frequency information. The final step is a simulation of trajectories based on the aircraft movements obtained from the aircraft movements network layer using DLR's Global Air Traffic Emissions Distribution Laboratory (GRIDLAB; Linke, 2016). Each mission, defined by departure and arrival cities, aircraft type, and load factor, was simulated under typical operational conditions, resulting in a network of flight trajectories. For this purpose, DLR's Trajectory Calculation Module (TCM; Lührs et al., 2014) was used that applies simplified equations of motion known as the Total Energy Model.

Based on the aircraft's engine state determined by parameters such as thrust and fuel flow, the engine emission distribution of NO_x, CO, and HC species along the trajectory was determined by applying the Boeing Fuel Flow Method 2 (DuBois and Paynter, 2006). The amount of CO_2 and H_2O emissions was calculated assuming a linear relationship to the fuel burn. The mapping of emission distributions of all flights onto a geographical grid resulted in 3-D inventories. In WeCare, using the approach mentioned above, emission inventories and the corresponding climate effect were estimated for the years 2015 to 2050 in 5-year steps. The forecast was based on the dataset from the reference year 2012. Seven different aircraft seat categories (based on the number of seats) were considered in the inventories (20-50 seats; 51-100 seats; 101-151 seats; 152-201 seats; 202-251 seats; 252-301 seats; 302-600 seats). Each seat category was modeled using one representative jet powered aircraft type (plus one backup aircraft type). The representative aircraft type was selected such that it contributes to a significant share of the respective seat category. Respective engine emission characteristics were taken from the Aircraft Engine Emissions Databank of the International Civil Aviation Organization (ICAO, 2023).

2.2 Climate effect estimation

In order to obtain the climate effect for each flight corresponding to the flight plan, the climate effect for the emissions calculated along each single trajectory is estimated with the non-linear climate response model AirClim (Grewe and Stenke, 2008; Dahlmann et al., 2016a) using gridded emission data for each species. Therefore, AirClim combines 3-D aircraft emission data with a set of pre-calculated non-linear emission–response relations for a set of atmospheric locations to estimate the temporal development of the global near-surface temperature change. AirClim includes the effects of the climate agents CO_2, H_2O, CH_4, O_3 and primary mode ozone (PMO) (the latter three result from NO_x emissions), as well as CiC. For deriving the atmospheric responses for H_2O and NO_x-induced changes, 85 steady-state simulations for the year 2000 were performed with the chemistry climate model E39/CA (Stenke et al., 2009), prescribing normalized emissions of NO_x and H_2O at various atmospheric regions (Fichter, 2009). For the effect of CiC, we use atmospheric and climate responses considering the local probability of fulfilling the Schmidt-Appleman criterion as well as ice-supersaturated regions, which were obtained from simulations with ECHAM4-CCMod (Burkhardt and Kärcher, 2011). We follow a climatological approach in the estimation of

the climate effect, meaning that the calculated values represent a mean over all weather situations averaging over individual spatially and temporally resolved responses.

For analyzing the climate effect, a physical climate metric is selected which assumes growing emissions for characterizing radiative effect of the single flight emission in a future atmosphere, instead of applying a pulse metric. The reason behind this choice is that there exists a mismatch between the summed effect of pulse emissions and the respective scenario analysis (equal to the effect of aggregated pulse emissions). Therefore, we calculate CO_2-equivalents based on a scenario with ATR100 as a metric and apply these equivalence factors to the pulse emissions in *FlightClim*. As a consequence, when selecting ATR100 as a physical climate metric, the climate effect of these single flight emissions is evaluated assuming a future increase of emissions and concentrations from future flights and future contributions from non-aviation sectors over the next 100 years. This is relevant for the radiative effects estimated as changing concentrations in the future are taken into account. Hence, we assume emissions starting in 2012 and a future increase in emissions according to the scenario Fa1 of the Intergovernmental Panel on Climate Change (IPCC, 1992), which is a reference scenario developed by the International Civil Aviation Organization Forecasting and Economic Support Group (ICAO FESG) with mid-range economic growth and technology for both improved fuel efficiency and NO_x reduction (IPCC, 1999). Historical emissions are neglected. For background concentrations of CO_2 and CH_4, which influence the climate effect of CO_2 and CH_4 emissions, we assume IPCC scenario RCP4.5 (Meinshausen et al., 2011). A number of different climate metrics can be applied to account for the different components of the aviation climate effect. However, selecting a suitable metric is challenging due to the uncertainties and varying lifetimes of non-CO_2 effects. Megill et al. (2024) recommend using the average temperature response (ATR) or the efficacy-weighted global warming potential (EGWP) with a time horizon of more than 70 years. As a time horizon of 100 years was used for the Kyoto Protocol and other political applications, we quantify the climate effect using ATR100, which is the mean near-surface temperature change over 100 years. For any climate metric, non-CO_2 effects can be expressed as an equivalent amount of CO_2 emissions, so called CO_2-equivalents ($CO_{2,e}$), that would produce the same effect over a defined time horizon and a given emission scenario. Hence these CO_2-equivalents are derived from a scenario analysis and applied in *FlightClim* to a pulse emission to obtain the best possible consistency between the effects of pulses and the scenario.

AirClim does not account for the influence of different aircraft sizes on contrail climate effect. To account for that we use a parametrization derived from Unterstrasser and Görsch (2014) (see Sec. S1 in Supplementary Material). While this parametrization is already included in the ATR100-values used for the Symbolic Regression (see Sec. 3.2), the MR-formulas for CiC have to be scaled afterwards (see Sec. 3.1).

In the data structure for each of the about 57 thousand simulated flight trajectories, characterized by origin and destination airport as well as aircraft size, the resulting amounts of engine emissions were stored together with the ATR100 climate effect per species. This database was then used to derive the climate effect regression functions as well as regression formulas for fuel use and NO_x emissions necessary for the MR-approach.

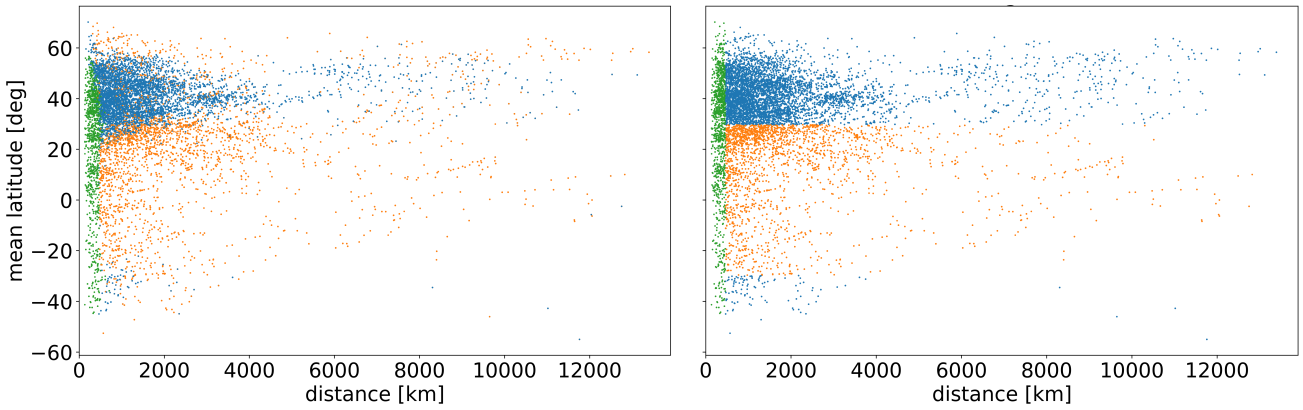

(a) Original clusters from K-Means.

(b) Clusters using simple thresholds.

Figure 2. Clustering of flights, as obtained by the K-Means clustering algorithm (a) and as delineated by simple thresholds (b), shown in the mean latitude–distance space. Each color corresponds to one cluster. We name them the short-flight cluster (green), the tropical cluster (orange), and the mid-latitude cluster (blue).

2.3 Clustering of flights by relative climate effects

Due to the large variety of importance of the different climate effect components among different flights, it is challenging to find a single set of equations that would reasonably estimate the climate effect under most circumstances. Therefore, in the first step, we apply a K-Means clustering algorithm to separate the flights into several clusters. This clustering is based solely on the share of the six aforementioned components of the climate effect in the total climate effect:

$$\frac{\mathrm{ATR100}_{\mathrm{CO_2}}}{\mathrm{ATR100}_{\mathrm{tot}}}, \frac{\mathrm{ATR100}_{\mathrm{H_2O}}}{\mathrm{ATR100}_{\mathrm{tot}}}, \frac{\mathrm{ATR100}_{\mathrm{CiC}}}{\mathrm{ATR100}_{\mathrm{tot}}}, \frac{\mathrm{ATR100}_{\mathrm{O_3}}}{\mathrm{ATR100}_{\mathrm{tot}}}, \frac{\mathrm{ATR100}_{\mathrm{PMO}}}{\mathrm{ATR100}_{\mathrm{tot}}}, \text{and } \frac{\mathrm{ATR100}_{\mathrm{CH_4}}}{\mathrm{ATR100}_{\mathrm{tot}}}.$$

This ensures that flights in a given cluster have similar climate effect characteristics. The clustering is not directly dependent on proxy quantities to the climate effect, such as the amount and location of the emissions. We use an implementation by the free software machine learning library for the Python programming language scikit-learn (Pedregosa et al., 2011) and scale the input quantities to the standard normal distribution before clustering. We find a partition into three clusters to be most useful, as larger numbers of clusters lead to some cluster distinctions lacking a clear physical interpretation. The resulting three clusters occupy distinct areas in the latitude-distance space (Fig. 2a). We therefore name them the short-flight cluster (green), the tropical cluster (orange), and the mid-latitude cluster (blue).

In the second step, simple thresholds are derived which separate the flights into three categories that approximate the found clusters. This is necessary to enable easy categorization of additional flights not contained in this data set. One threshold is a maximum distance for the short-flight cluster, and another threshold is the absolute mean latitude of great circle trajectories confining the tropical cluster. We choose the values for these thresholds in such a way that the amount of wrongly categorized flights is minimized. This leads to a threshold distance of 462.5 km below which flights are categorized as belonging to the

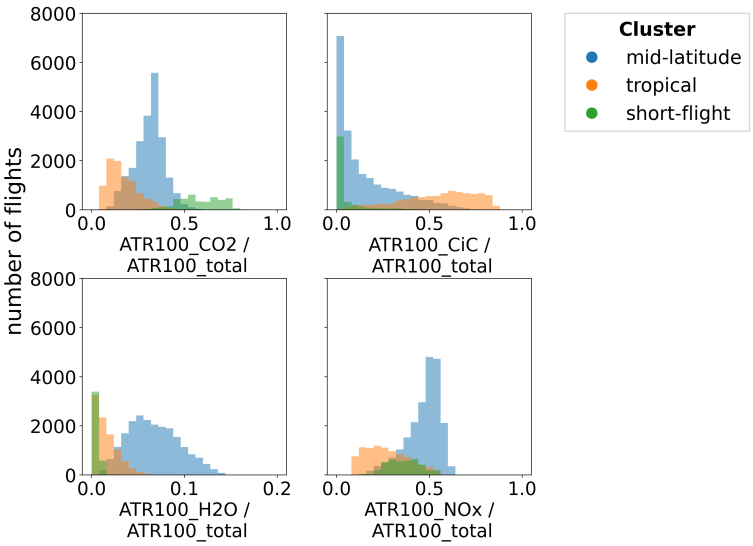

Figure 3. Number of flights as function of ratio of the individual climate effect components (CO_2, CiC, H_2O, and NO_x) to the total climate effect for the 3 flight clusters.

short-flight cluster, and a threshold mean latitude of $\pm 29.7°$ within which flights are categorized as belonging to the tropical cluster. All other flights are categorized into the mid-latitude cluster. This approximation wrongly categorizes 16.8% of all flights used for clustering. The resulting simplified clustering is shown in Figure 2b.

The three clusters have distinct characteristics (Fig. 3). The short-flight cluster has a negligible contribution of contrails to the climate effect at an average of 3.5%, and a strong contribution of CO_2 at an average of 57.4% of the total climate effect. Flights in this cluster are often too short to reach the required altitude of at least about $8\,\mathrm{km}$ (e.g.; Kärcher, 2018) for contrail formation. The climate effect of the tropical cluster is dominated by contrails (average contribution of 56.6%) because strong contrail formation occurs at tropical latitudes. The mid-latitude cluster contains the remaining flights and has large climate effect contributions from NO_x and H_2O (average contributions of 49.1% and 6.8%, respectively; see below for further discussion).

For the cluster analyses only flights with seat category 3 to 7 are used. The remaining seat categories 1 and 2 (less than 100 seats) were only added to the dataset later in development. They contribute only 4.2% to global ASK and therefore a minor share of total aviation emissions. Nevertheless the number of flights with seat category 1 and 2 is high. Therefore, an additional cluster for regional jets was used for MR. For SR all flights were clustered in one of the three clusters.

3 Derivation of climate effect regression functions

Based on the dataset described in Sec. 2, we derive climate effect regression functions for each emitted species (CO_2, NO_x, H_2O, as well as CiC) separately. These formulas use the size of the aircraft and the locations of departure and arrival airports

as input to quickly estimate of the climate effect of individual flights. We explore the use of both MR and SR models for easy-to-use climate effect estimation of individual flights. In the two regression analyses the following quantities are used: flight distance along a great circle d [km], mean latitude along the great circle $\bar{\phi}$ [°], fuel use f [kg], $\mathrm{NO_x}$ emissions e [kg], maximum takeoff mass (MTOW) m [kg], wing span b [m] and ATR100 [mK].

MR is a widely used statistical approach that models the relationship between a dependent variable (e.g., climate effect of $\mathrm{NO_x}$ emissions) and multiple predefined independent variables, called predictors. The functional relationship between the dependent variable and the predictors has to be predefined. Therefore this approach is especially useful when the factors influencing the climate effect of the single species are well-understood. However, the predefined functional form may fail to capture more complex, non-linear interactions between variables. On the other hand, SR is an advanced technique that searches for the best mathematical expression to describe the data, offering greater flexibility and the potential to uncover hidden relationships. While SR can model highly complex, non-linear interactions, it requires more computational resources and bears the peril of overfitting. By applying both methods, we aim to identify the approach that most effectively models especially non-$\mathrm{CO_2}$ effects, while prioritizing solutions that offer better accuracy and easy interpretability.

For both methods, we derived regression functions that approximate the climate effect for a particular flight as estimated by using the AirClim model. Following Dahlmann et al. (2023), the total climate effect as expressed by ATR100 can be obtained by the sum of the effects from the individual climate agents, where $\mathrm{ATR100_{NO_x}} = \mathrm{ATR100_{O_3}} + \mathrm{ATR100_{PMO}} + \mathrm{ATR100_{CH_4}}$ is the combined climate effect of $\mathrm{NO_x}$ emissions:

$$\mathrm{ATR100_{tot}} = \mathrm{ATR100_{CO_2}} + \mathrm{ATR100_{H_2O}} + \mathrm{ATR100_{CiC}} + \mathrm{ATR100_{NO_x}} \tag{1}$$

3.1 Multiple Regression formulas

Multiple Regression is a common method in environmental science, with primary advantages being its simple application and interpretability. The structure of MR functions is predefined as a sum of predictor dependent terms each multiplied by a coefficient. Each coefficient indicates the impact of a specific predictor, allowing to understand the effects of each variable on the climate. It also enables the inclusion of numerous variables and can incorporate interaction terms of multiple predictors. However, MR assumes a predefined mathematical form making knowledge about the interactions necessary, which can be a limitation when relationships are non-linear. The necessary assumption may lead to misspecification of the model if the actual relationships are not well-captured by these forms. Additionally, MR can be vulnerable to multicollinearity (when predictors are highly correlated), which can distort coefficient estimates.

The MR-approach extends the idea of Dahlmann et al. (2023) and leads to the following structure for the derived formulas for all clusters:

$$\mathrm{ATR100_{tot}} = c_{\mathrm{CO_2}} \cdot f + c_{\mathrm{NO_x}}(d, \bar{\phi}) \cdot e + c_{\mathrm{H_2O}}(d, \bar{\phi}) \cdot f + c_{\mathrm{CiC}}(d, \bar{\phi}) \cdot d \cdot f_{ACsize}(b)\,, \tag{2}$$

where f_{ACsize} is the adaptation factor for the contrail climate effect due to the wing span b (see Eq. S2 in Supplementary Material), and $c_{\mathrm{CO_2}}$, $c_{\mathrm{NO_x}}$, $c_{\mathrm{H_2O}}$, c_{CiC} are the cluster-dependent climate effect regression functions. Therefore, the climate effect of a species is estimated as a product of the respective climate effect regression function and the relevant reference quantity (f, e,

$d \cdot f_{ACsize}$) . These MR-formulas are composed of polynomial and arctan functions and are designed to fit the respective partial climate effects $c_{\mathrm{CO_2}}$=ATR100$_{\mathrm{CO_2}}/f$, $c_{\mathrm{NO_x}}$=ATR100$_{\mathrm{NO_x}}/e$, $c_{\mathrm{H_2O}}$=ATR100$_{\mathrm{H_2O}}/f$, and c_{CiC}=ATR100$_{\mathrm{CiC}}/d$. The climate effect function for $\mathrm{CO_2}$ is fixed at $c_{\mathrm{CO_2}} = 8.145 \times 10^{-11}\mathrm{mK/kg(fuel)}$, because the climate effect of $\mathrm{CO_2}$ is independent of the emission location in AirClim, so that no fit is required. Details on the derivation of the MR-formulas are given in Section S2.2 in the Supplementary Material.

Note that for the derivation of the climate effect regression functions apart from the predictors d and $\bar{\phi}$ we use the WeCare estimates for the burnt fuel f and emitted $\mathrm{NO_x}$ e, implying that those are also required for the application of these formulas. If those are not available we provide additional Fuel and $\mathrm{NO_x}$ MR functions, that only use the flight distance d and seat category (S2.1 in Supplementary Material). For the comparison with the SR-approach in Section 3.4 the derived Fuel, $\mathrm{NO_x}$ and climate effect regression functions are considered, combined determining the quality of the climate effect estimation.

3.2 Symbolic Regression formulas

The Symbolic Regression method used here, avoids a pre-defined structure of the formula. Instead an evolutionary algorithm provides a best fit and thereby defines the structure of the formulas. This structure can be represented by an expression tree, called gene. Each node in the gene represents a variable, a mathematical operation or a constant. The nodes are merged to a formula by the tree structure (Koza, 1992). The tool we apply, GPTIPS 2 (Searson, 2015), specifically uses Multi-Gene Symbolic Regression, which combines multiple genes with an additional scaling factor per gene (b_1, b_2) and a bias term (b_0) to assemble the whole formula (Fig. 4).

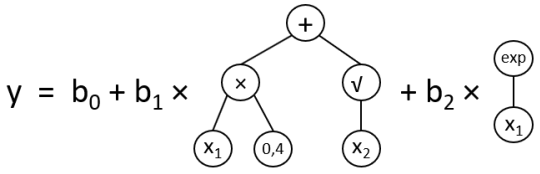

Figure 4. Structure of a Multi-Gene Symbolic Regression formula consisting of two genes with factors (b_1, b_2) and a bias term (b_0).

The optimization process to find an optimal formula uses an evolutionary algorithm based on a fitness function, in this case the root mean square error for the given dataset. Beneficiary solutions based on a random start population of multiple formulas are evolved over several generations. The evolution-inspired mechanisms forming the final formulas are fitness-based selection, as well as mutation and crossover (Koza, 1992).

For the derivation of regression functions the flight database is split into 80% training and 20% test data. Four different formulas are computed for the climate effect of the climate agents $\mathrm{CO_2}$, $\mathrm{H_2O}$, $\mathrm{NO_x}$, and CiC (see Eq. 1). The two main predictors, d and $\bar{\phi}$ from the first approach are used in the second one as well complemented by m, that replaces the segmentation into seat categories. The flight distance d is meant to cover effects based on the flight length like fuel use, $\bar{\phi}$ geographically differing climate effects of emissions and m different aircraft sizes. The dependent variable of the SR-formulas is the ATR100 for $\mathrm{CO_2}$, $\mathrm{H_2O}$, CiC and $\mathrm{NO_x}$.

To check the effectiveness of the clustering derived in Sect. 2.3, regression formulas with and without use of the three clusters are computed. In the clustered version, separate formulas are derived for each cluster. This leads to in total twelve formulas for the clustered version and four for the unclustered one. For each resulting formula of the clustered and unclustered version a multiple runs of GPTIPS 2 (1296 for unclustered and 648 for clustered) are executed as part of a gridsearch for the regression hyperparameters. The main settings of the GPTIPS-software are used as hyperparameters. The reason for the selected gridsearch-approach with many runs is the high variability in the resulting estimation quality of regression formulas.

From all derived formulas the Pareto-optimal individuals according to the coefficient of determination R^2 (Eq. 3) and the number of nodes are considered as candidates for the final formula of the species and cluster (see Sec. S3.1 in Supplementary Material). To obtain one formula for the total climate effect the formulas for CO_2, H_2O, CiC and NO_x have to be combined according to Equation 1. In this step the numbers of nodes for the $ATR100_{tot}$ add, but the quality of estimation measured as R^2 has to be newly computed. It is not apparent, which Pareto-formula to choose for each species to achieve an optimum in estimation quality and number of nodes for $ATR100_{tot}$. However, by trying all combinations it is possible to identify Pareto-optimal combinations that represent a optimal trade-off between a high value of R^2 and a low number of nodes. Figure 5 shows these $ATR100_{tot}$-Pareto-fronts for the unclustered (blue) and the aggregated clustered version (purple; for the individual clusters please see the Supplementary Material, Figure S9). The final choices made are indicated by red and green dots. The selected formulas are given in the Supplementary Material in Section S3.1.

$$\mathrm{R}^2 = 1 - \frac{\sum_{i=1}^{N}(\mathrm{ATR100}_{\mathrm{tot}}^{\mathrm{pred}} - \overline{\mathrm{ATR100}_{\mathrm{tot}}^{\mathrm{act}}})^2}{\sum_{i=1}^{N}(\mathrm{ATR100}_{\mathrm{tot}}^{\mathrm{act}} - \overline{\mathrm{ATR100}_{\mathrm{tot}}^{\mathrm{act}}})^2} \tag{3}$$

For $ATR100_{tot}$ in the short-flight cluster the clustered approach shows a significantly better estimation quality than the unclustered one (see Supplementary Material, Fig. S10). For the two other clusters the quality is comparable. Therefore as a combination of low complexity and a high quality of estimation the clustered formulas are applied for flights in the short-flight cluster in the further analysis and the unclustered formulas are used for mid-latitude and tropical cluster flights.

3.3 Smoothing of regression formulas at the cluster boundaries

The use of different regression formulas for the derived clusters leads to discontinuities at the cluster boundaries that do not reflect real behavior and might result in inconsistencies. The significant difference in estimated climate effect over the cluster boundaries (e.g. see Fig. 6) makes it necessary to smooth this effect. The smoothing is implemented by using a weighted sum of the cluster-specifically computed climate effects. The weighting factor evolves linearly from a starting point inside the particular cluster until the cluster boundary. At the cluster boundary the weighting of both cluster formulas is equal. Figure 7 sketches this general scheme of the smoothing. The climate effect of a flight within the smoothing area is accordingly estimated by

$$\mathrm{ATR100} = \begin{cases} \mathrm{ATR100}_{C1} \cdot (0.5 + \frac{|d_{C1,2}|}{2 \cdot b_{C1}}) + \mathrm{ATR100}_{C2} \cdot (0.5 - \frac{|d_{C1,2}|}{2 \cdot b_{C1}}), & \text{if } d_{C1,2} \in [-b_{C1}, 0[\\ \mathrm{ATR100}_{C1} \cdot (0.5 - \frac{|d_{C1,2}|}{2 \cdot b_{C2}}) + \mathrm{ATR100}_{C2} \cdot (0.5 + \frac{|d_{C1,2}|}{2 \cdot b_{C2}}), & \text{if } d_{C1,2} \in [0, b_{C2}], \end{cases} \tag{4}$$

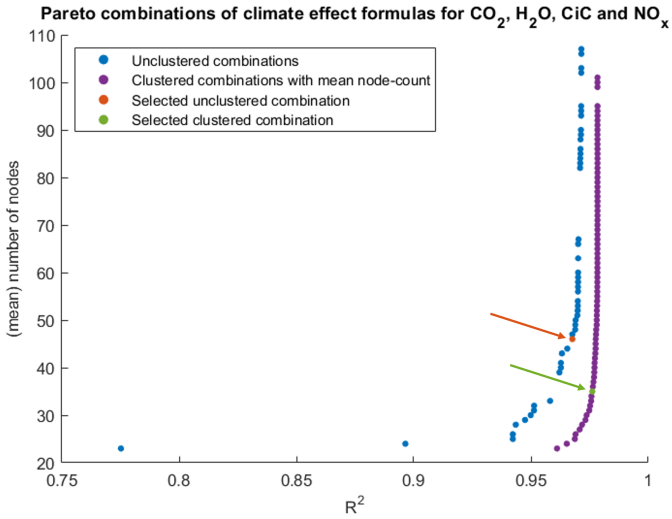

Figure 5. Pareto-optimal solutions for a Symbolic Regression of the climate effects with respect to R^2 and number of nodes by using the unclustered data (blue) and a combined pareto-front of the clustered data (purple). The pareto-optimal solutions, that are chosen, are indicated in red and green.

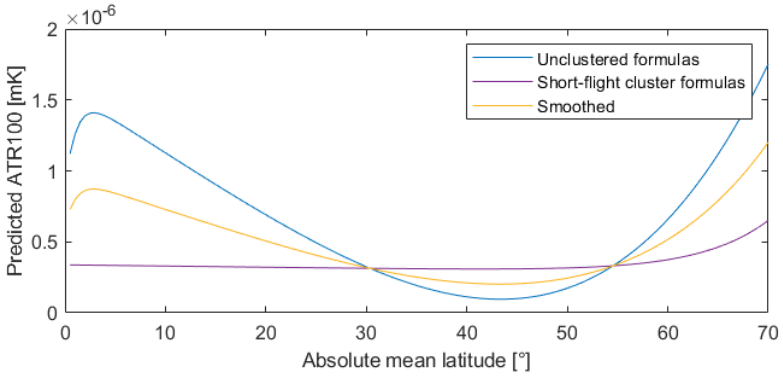

Figure 6. ATR100 estimates for flights with an Airbus A320 over the cluster boundary distance of 462.5km depending on the mean latitude. The plot shows the estimation with the unclustered SR-formulas, the formulas for the short-flight cluster as well as the smoothed version, taking the mean of the partially largely differing estimates.

with $\mathrm{ATR100}_{C1}$/$\mathrm{ATR100}_{C2}$ as the cluster 1 / 2 estimates, $d_{C1,2}$ the distance from the cluster boundary and b_{C1}/b_{C2} the smoothing boundary 1 / 2 values. The smoothing boundaries mark the starting points of the smoothing area and are derived as the R^2-optimal values within preset boundaries.

For both approaches smoothing is applied to the existing cluster boundaries of the recommended versions. The details on the individual smoothing are outlined in the Supplementary Material in the Sections S2.3 and S3.2.

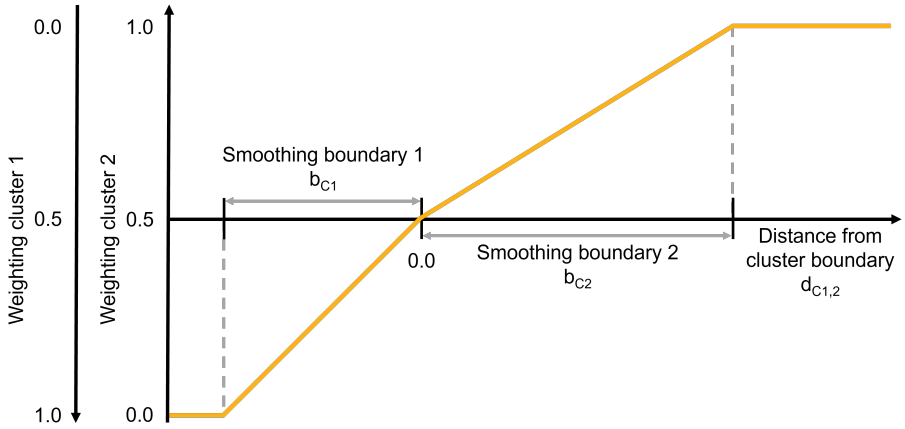

Figure 7. Concept for smoothing of regression results at cluster boundaries. The smoothing takes place linearly in a predefined range (smoothing boundary) on both sides of the cluster boundary.

3.4 Comparison of climate effect regression approaches

The climate effect functions were developed to represent a fitting of more detailed results from the non-linear response-model AirClim with algebraic relationships. Hence, the reliability of representing the estimated total climate effect is influenced by the applied fitting procedure. To evaluate the quality and reliability of the estimates, the derived, smoothed formulas from MR and SR are compared in this section. For SR, the formulas estimate the $\mathrm{ATR100}$ directly leading to one formula per cluster and species. For MR the climate effect functions have to be computed for each cluster, which are four formulas per species apart from $\mathrm{CO_2}$, on the one hand, as well as the regression formulas for the used reference quantity on the other. Those are seven formulas for the fuel regressions, one per seat category, and 14 formulas for the $\mathrm{NO_x}$ regressions, two per seat category. The last formula of the MR-approach is the subsequent contrail wing span adaption. In total, this leads to 35 formulas for MR compared to 8 formulas for SR without smoothing (see Tab. 1).

One advantage of the MR-approach are the separate fuel and $\mathrm{NO_x}$ functions, which the SR-approach does not include directly, hence fuel can still be derived from the $\mathrm{CO_2}$ climate effect. Furthermore all MR-formulas have the same predefined structure, while each SR-formula is different in shape and operators. Also, even though the SR-approach is optimized towards minimum formula complexity, it generally tends to include irrelevant, over-fitting terms and does not include certain input parameters into formulas for species, where correlations are present (e.g. $\bar{\phi}$ into $\mathrm{ATR100_{NO_x}}$). As advantages the SR-approach evolves according the optimum predictive accuracy and yields a better ratio of complexity in terms of the number of formulas to quality. In addition it enables a continuous estimation over the aircraft size by using the MTOW instead of categorical seat categories. The number of formulas and the input parameters are a result of the different study designs for the two approaches and not inherent to the methods, even though the SR approach supports a lower number of formulas by being able to adapt to complex dynamics independently, whereas the MR-approach depends on a predefined structure. Therefore the

Table 1. Comparison of Multiple Regression and Symbolic Regression formulas for the estimation of the climate effect of individual flights. Quality of fit is quantified by R^2 and MARE. Due to zero or almost zero values in the dataset MARE is not defined for $\mathrm{ATR100_{H_2O}}$ and $\mathrm{ATR100_{CiC}}$. The number of formulas is counted before smoothing. The first value is the number of formulas for the climate effect estimation and the second for supporting equations like the fuel and $\mathrm{NO_x}$-regressions.

Regression formulas		R^2	MARE	number of formulas
$\mathrm{ATR100_{CO_2}}$:	MR:	0.9972	5.03%	1 + 7
	SR:	0.9940	5.86 %	2
$\mathrm{ATR100_{H_2O}}$:	MR:	0.8613	-	4 + 7
	SR:	0.9233	-	2
$\mathrm{ATR100_{NO_x}}$:	MR:	0.9529	13.38 %	4 + 21
	SR:	0.9807	20.23 %	2
$\mathrm{ATR100_{CiC}}$:	MR:	0.8960	-	4 + 1
	SR:	0.8868	-	2
$\mathrm{ATR100_{tot}}$:	MR:	0.9619	20.71%	35
	SR:	0.9684	25.82 %	8

MR-approach features separate seat categories and a separate estimation of fuel consumption and $\mathrm{NO_x}$-emissions to distinguish their dynamics.

The estimation quality of both approaches is similar (Tab. 1). Overall, the SR-formulas show a slightly higher coefficient of determination R^2 (Eq. 3). This might result from the optimization towards R^2 in the SR-approach, even though for $\mathrm{CO_2}$ and CiC the MR-formulas show a slightly greater R^2. In terms of the mean absolute relative error (MARE; Eq. 5) the MR-formulas surpass the SR ones. This mainly results from the better relative estimation for short and medium range flights compared to the long range flights (see Fig. 8). The better estimation of longer flights of the SR-formulas is a result of the absolute error-based evolutionary optimization process, which gives a greater weight to longer flights with higher climate effect. The MARE for $\mathrm{H_2O}$ and CiC cannot be calculated due to flights with almost or exactly zero ATR100 in the dataset distorting the relative metric.

$$\mathrm{MARE} = \frac{1}{N}\sum_{i=1}^{N}\left|\frac{\mathrm{ATR100_{tot}^{act}} - \mathrm{ATR100_{tot}^{pred}}}{\mathrm{ATR100_{tot}^{act}}}\right| \tag{5}$$

The MARE of the climate effect estimation is generally higher for short flights, as for these the variety in flight trajectories and non-$\mathrm{CO_2}$-effects generation increases (Fig. 8). The correlation of both approaches with the AirClim estimated values is shown in Figure 9 (for MR) and 10 (for SR). For the estimation of $\mathrm{ATR100_{CO_2}}$ the MR-formulas show a better performance

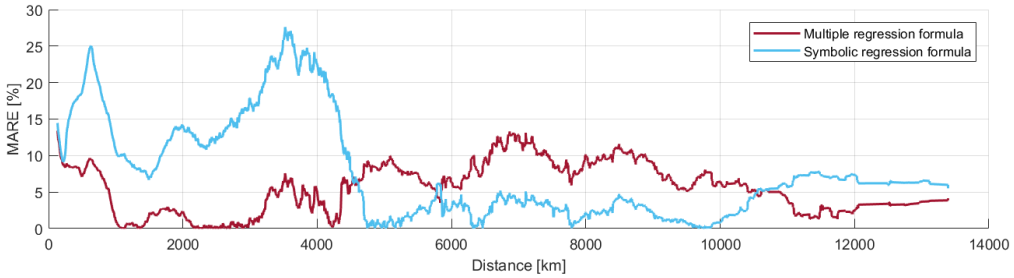

Figure 8. Trend comparison of the MARE for the $\mathrm{ATR100_{tot}}$ estimation with the Multiple and Symbolic Regression approach over the flight distance.

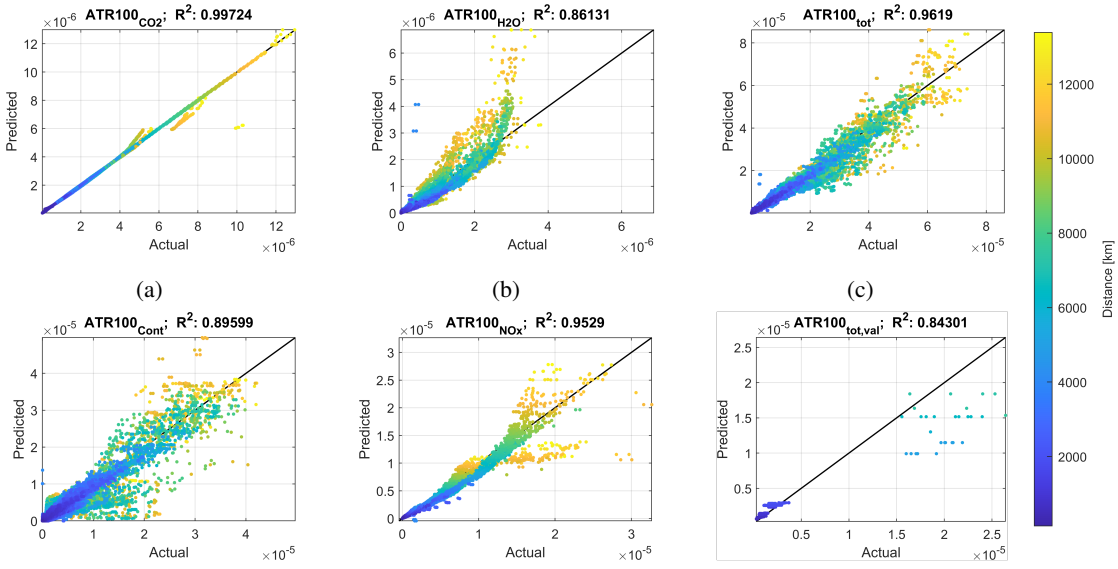

Figure 9. For Multiple Regression, correlation of estimated ATR100 of CO_2- (a), H_2O- (b), NO_x-emissions (e) and produced contrails (d) with the AirClim estimates (referred here as to "actual"), as well as the $\mathrm{ATR100_{tot}}$-estimation for the dataset (c) and a validation dataset (f). The color code indicates the flown distance.

than those of the SR-approach, especially for long distance flights, because the points in plot 9a are located closer to or almost on the diagonal compared to plot 10a. The SR-formulas generally tend to underestimate those flights with two noticeable groups of flights being overestimated. These two groups are also distinguishable in the MR-plot 9a. One of them is estimated better and the smaller one is instead underestimated.

$\mathrm{ATR100_{H_2O}}$-estimation (see plots 9b and 10b) shows relevant differences between both approaches with the MR-formulas generally overestimating the climate effect especially for long flights. The SR-formulas show a better accuracy for those flights and do in general neither tend to over- nor underestimate.

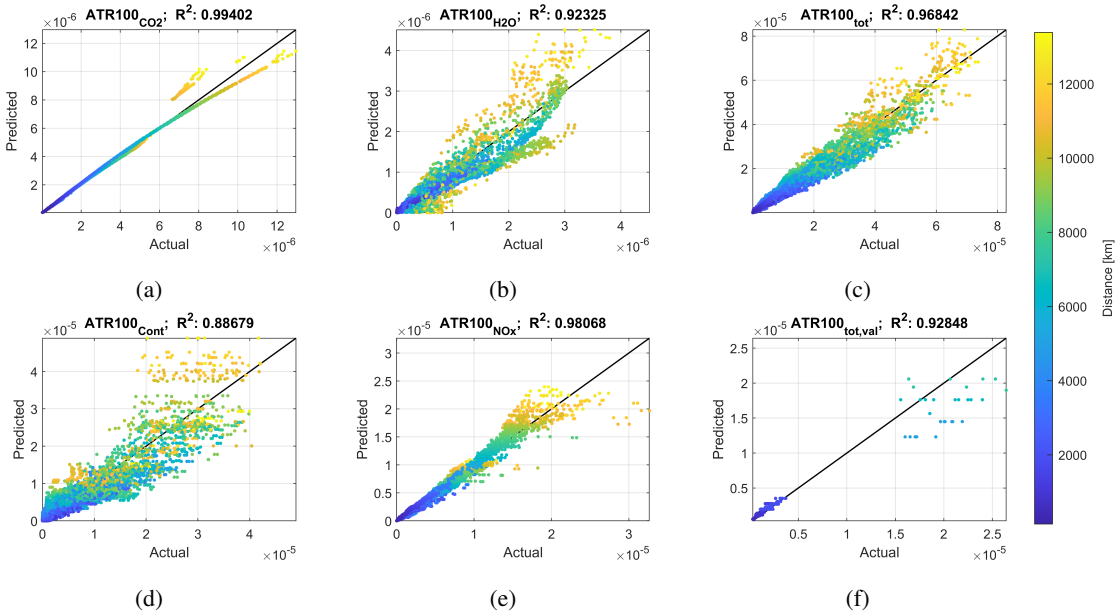

Figure 10. Same as Figure 9 for Symbolic Regression.

The quality of estimation for the climate effect of contrails is similar for both approaches (see plots 9d and 10d). As the occurrence of contrails is hard to predict and model, the accuracy of the CiC formula is low. The calculation of a meaningful MARE for contrails is not possible for short flights due to some flights with zero or close to zero ATR100 values, but for longer flight distances the MARE is by 2 to 4 times higher than that of $\mathrm{ATR100_{tot}}$.

For $\mathrm{ATR100_{NO_x}}$ the SR-approach leads to a better quality of estimation, with fewer points far away from the diagonal in plot 10e than for MR in plot 9e, indicating fewer large estimation errors. In contrast to the SR-formulas the MR-formulas have a tendency to under- or overestimate some distinguishable groups of flights.

The $\mathrm{ATR100_{tot}}$ correlations in plots 9c and 10c show only minor differences between the two approaches. Hence we can conclude that the total quality of both approaches is similar, only with certain advantages for single species.

Apart from the results for the used dataset, the performance of the estimated $\mathrm{ATR100_{tot}}$ for a validation dataset is analyzed. The validation dataset includes 439 flights of the German cargo airline EAT. The mainly short and medium haul flights took place with Airbus A300, A330 and Boeing 757 aircraft in 2021 and 2022. The AirClim climate effect estimates based on the real trajectories of these flights serve as the validation reference. The formulas of both approaches show reasonable correlations for the validation dataset, indicating a valid estimation. Longer flights are rather under- than overestimated (see plots 9f and 10f). This trend is stronger for the MR-formulas, which do also have a lower R^2 value for the validation dataset.

Assessing the sum of all ATR100 estimates for the regression dataset shows the SR-approach to be closer to the actual AirClim values than the MR-estimates. The sum of MR-approach estimates is, apart from $ATR100_{H_2O}$, in average smaller than the actual values, which results in the total sum of ATR100 estimates being 5.4 % smaller than the sum of all actual AirClim estimates. For SR the estimated sum is 0.3 % greater than the actual sum. The median signed relative error shows a

different trend for both approaches, as it indicates a median relative overestimation of 0.6 % for MR, while SR-formulas in median overestimate by 9.8 %, mainly caused by many overestimated short flights with larger relative errors. This indicates different characteristics for different group of flights of different total amounts of climate effect. But in total about half of the flights are over- and half of them are underestimated for the MR-approach, while for the SR-approach about two third of the flights are overestimated.

4 FlightClim v1.0 implementation

The derived regression models from MR are implemented in an Excel application called *FlightClim v1.0*, which is available in the Supplementary Material. *FlightClim* offers an easy-to-use estimation of CO_2 and non-CO_2 climate effects solely based on the aircraft size, as well as origin and destination airports without further knowledge about the actual flight conditions. *FlightClim´s* core is a simple, tabular input mask supporting the estimation of single flights as well as whole flight plans. Thereby, the tool is suited for individuals estimating the climate effect of a holiday trip, organizations assessing their one year carbon footprint, but also airlines approximating the climate effect of their flight plan.

After a selection of input values in the input mask (climate metric; aircraft size; origin and destination airports; optional: flight frequency and flight class), the interactive tool returns the climate effect of a flight for CO_2, H_2O, NO_x emissions and CiC in the selected metric and as CO_2-equivalents. If a flight class is entered, *FlightClim* also calculates a statistically backed allocation per passenger (see Sec. S4 in Supplementary Material). In addition to the climate effect, the fuel burn estimate as well as the estimated CO_2 and NO_x-emissions are returned as intermediate results of the MR-formulas. The interpretation of the inputs is based on two tool-integrated databases for airport coordinates and aircraft characteristics. In the Supplementary Material in Section S7 the user guide of the tool is included.

In *FlightClim* the MR-formulas are implemented. Compared to the SR-formulas they show a slightly better quality of estimation for short- and medium-haul flights, which are dominating long-haul flights in number. In addition the tool´s main area of application is seen in Europe, where inner-European short- and medium-haul flights are dominant. The one-time implementation of the MR-formulas makes their greater complexity in terms of number of formulas less relevant. An extended version of *FlightClim* contains the models of both regression approaches and is available upon request, but less suited for ordinary use, due to the necessary choice of model.

5 Discussion

One of the key aspects of our work is that aviation emissions have different effects depending on their emission location and characteristics. *FlightClim* tries to model the high-level effects with a regression model. In the regression dataset the sensitivity of the atmospheric response is represented by AirClim and the underlying response surfaces, whereas the emission characteristics are given by the aircraft/engine combination and the flight route. This leads to spatially and technologically varying non-CO_2 to CO_2 ratios in the estimation. In Section 5.1 we discuss the developed estimation models and especially also

this factor in more detail. In Section 5.2 we concentrate on uncertainties in the calculation and in Section 5.3 on *FlightClim's* applicability.

5.1 Estimation of flight climate effect

The goal of this study is to develop an easy-to-use calculation method for estimating the total climate effect of individual flights, including CO_2 and non-CO_2 effects. Two approaches with smoothed formulas from MR and from SR have been compared. Due to the similar estimation quality of both approaches their greatest differences are the number of formulas and the input parameters, which can hence serve as crucial points for making a choice. Therefore, the SR-formulas can be recommended for application, if the complexity of the calculation in terms of the number of formulas is an important factor or if the aircraft size should be modeled continuously. If the estimation quality of short- and medium-haul flights is of greater importance, like for the *FlightClim* implementation, the MR-formulas are the better choice. In general, the specific requirements of an application towards the complexity, interpretability or the quality of estimation should serve as decisive points, which approach to use.

For both approaches applied in this study the ratio between non-CO_2 and CO_2 effects is approximately 4 for the used global aviation emission dataset. This number is higher than in other alternative publicly available methods for simplified climate footprint assessment of single flights. They use a constant factor of 2 to 3, which is based on assessments of total historical aviation emissions (e.g., from 1940 to 2018 for Lee et al., 2021), which is in principle consistent with AirClim results (see Sect. 5.2). It has to be noted that the relation between non-CO_2 and CO_2 strongly depends on the level of the CO_2 reference and the climate metric. Since the regression functions are designed to estimate the climate effect of present and future flights, we do not consider any emissions of historic aviation. Given the long lifetime of CO_2, historical assessments such as Lee et al. (2021), who analyzed aviation emissions from 1940 to 2018 in terms of ERF, report a stronger dominance of CO_2 (31%) than in the present study (19%). A direct comparison is, however, limited because different metrics (ATR vs. ERF) and emission patterns (historical vs. present and future) are considered. Nevertheless, the relative importance of non-CO_2 species is broadly similar, with shares of 4 % for H_2O, 33 % for NO_x and 44 % for CiC in our dataset versus 2 % for H_2O, 16 % for NO_x and 52 % for CiC in Lee et al. (2021), when excluding the studied aerosol effects.

5.2 Uncertainties in the estimation of flight climate effects

Clearly, aviation non-CO_2-effects are subject to large uncertainties. The uncertainties regarding the climate effect of individual routes as described here, are likely to be even larger than those for the global average. Here we conceptually (and mathematically) distinguish between uncertainties in the importance of individual aviation effects that are globally applicable (global uncertainty) and the sensitivity of these effects to certain influences like location or aircraft technology (differential uncertainty). This discrimination is shown in Figure 11 that describes a full approach in assessing uncertainties in the climate effect of individual flights estimated with *FlightClim*. Figure 11 is based on the high-level modeling workflow of *FlightClim* as illustrated in Figure 1 (grey box).

We start by considering a one-year 3-D emission inventory, as usually done in climate effect assessments, and derive the climate response to individual flights by using AirClim that is based on athmospheric response surfaces derived from chemistry

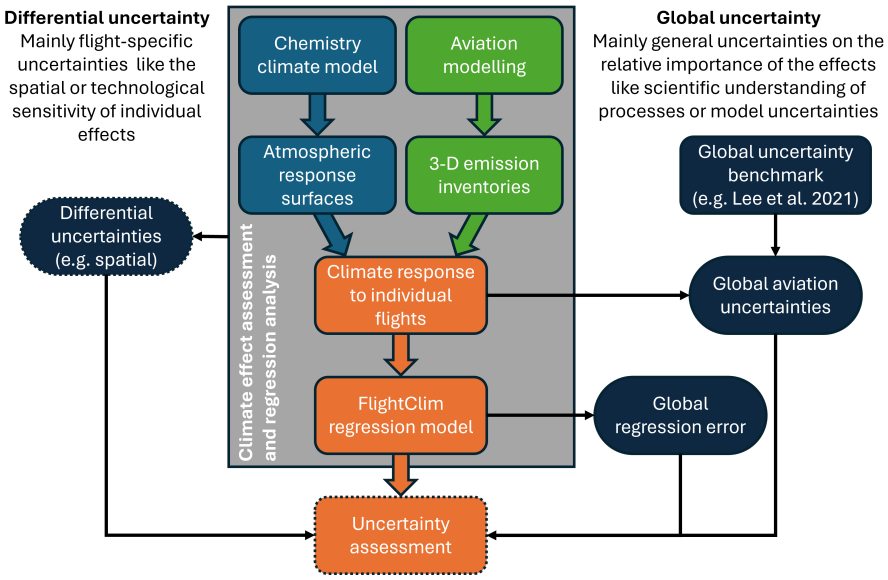

Figure 11. Sketch of a full uncertainty assessment for *FlightClim*. Light blue, green, orange and dark blue boxes mark atmospheric, aviation, combined and uncertainty related processes and steps.

climate model simulations. Overall assessments of aviation climate effect, such as that from Lee et al. (2021) may serve as an uncertainty estimate for the importance of individual effects that basically represents the uncertainty in the ratio of CO_2 to individual non-CO_2 effects. Note that in the calculation of the uncertainty ranges in such assessments, different models are applied that are characterised by different spatial sensitivities. The main point here, however, is to distinguish between globally applicable uncertainty estimates and the effects of certain influences (differential uncertainty) like spatial variations. The approach applying globally applicable uncertainty estimates for individual flights has been used recently by Prather et al. (2025) and is applied to our results to derive global uncertainties in the applied aviation climate effect modeling.

In Figure 11, the global part in the uncertainty description is complemented by an assessment of flight-specific, here called differential, uncertainties like the spatial sensitivity of the responses or the influence of differences in aircraft technology, which requires a much more detailed analysis than merely estimating globally applicable values. In addition, only limited data of the uncertainties in those sensitivities is available. A detailed analysis is clearly beyond the scope of this work. Therefore, in the following, we concentrate on the first part only, bearing in mind that the differential uncertainty is not represented.

As we break down the overall mean effect into contributions from individual routes also opposite should apply for the uncertainties: The sum of the uncertainties of the climate impact from individual routes should result in the overall uncertainty of the best estimate e.g. as given in Lee et al. (2021). The regression formulas always try to model the median estimate. However, this might differ from median estimates in assessments (Sec. 5.1). Hence, for the estimate of the 90% confidence interval, we apply a mapping to the Lee et al. (2021) data, before applying those confidence interval globally to the *FlightClim* estimates. For the mapping from AirClim to the Lee et al. (2021) median we use reported data for estimates of the 2005 radiative

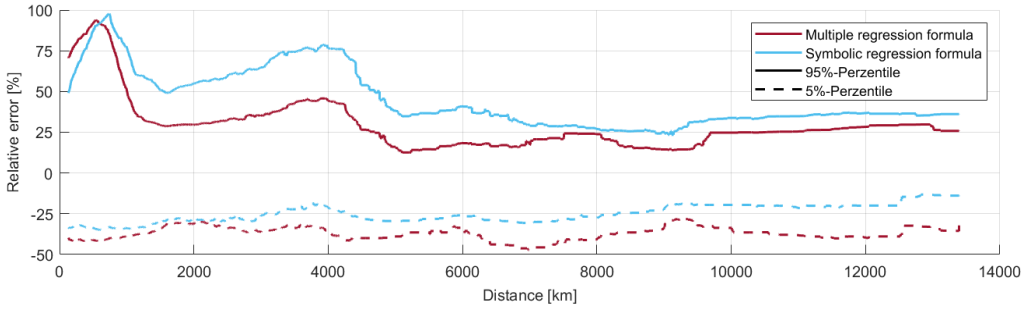

Figure 12. Confidence interval (90 %) of the relative error for MR and SR regression approaches over flight distance.

forcing (RF) (Grewe et al., 2021; Lee et al., 2021) and for the confidence interval ERF 2018 data (Lee et al., 2021) (Eq. 6 and Supplementary Material section S5 for more details). Hence, this approach guarantees a consistency of the confidence interval with values from Lee et al. (2021), while the actual calculated value represents the AirClim's best estimate including its spatial sensitivity. The CO_2 as well as the total RF AirClim estimate fits well with that of Lee et al. and the 90%-confidence interval is roughly $\pm$50%. However, AirClim's contrail and water vapor RF is lower and the ozone and PMO effect are greater than those from Lee et al.

$$\begin{aligned} \text{confidence interval (low/high)} &= ATR_x \times \frac{RF_x^{L21}}{RF_{AirClim}^{G21}} \times \frac{ERF_x^{L21}(low/high)}{ERF_x^{L21}} \\ &= ATR_x \times r_x^{ref} \times r_x^{L21}(low/high) \\ &= ATR_x \times r_x^{tot}(low/high) \end{aligned} \tag{6}$$

The second part of global uncertainties of the *FlightClim* estimates is the regression error, which adds on the before described uncertainty of the regression database. In this section we expand the analysis on the regression error from section 3.4, where the MARE and R^2 of the two applied regression approaches, MR and SR was discussed. To analyse the uncertainty of the regression the 90 % confidence interval of the relative error of the total ATR100 *FlightClim* result is calculated based on all flights in the regression dataset. Figure 12 shows that the 95 %-percentile varies over the length of flights for both regression approaches in a similar manner. The percentiles vary for short- (<1000 km) medium- (1000 km - 4500 km) and long-range (>4500 km) flights (see Table 2). While short-range flights have a larger confidence interval of the relative error of roughly -40 % to 80 %, the others are mostly in the range of $\pm\frac{1}{3}$.

5.3 Applicability of FlightClim

The derived MR-formulas are integrated into the easy-to-use Excel-tool *FlightClim v1.0*. When applying the estimator it is of key importance to consider its limitations. *FlightClim* is based on regression formulas, that fit the results of the climate response model AirClim, which is itself derived from chemistry-climate model simulations. This means that the estimation

Table 2. Confidence interval (90% ranging from the 5 %- to 95 %-percentile) for both regression approaches (MR & SR) in terms of the relative regression error for the estimated total ATR100 sectioned according to great circle flight distance d.

Relative regression error		d < 1000 km	1000 km ≤ d < 4500 km	4500 km ≤ d
MR:	5 %-percentile:	- 40 %	- 35 %	- 38 %
	95 %-percentile:	81 %	32 %	19 %
SR:	5 %-percentile:	- 33 %	- 30 %	- 27 %
	95 %-percentile:	80 %	60 %	33 %

quality and precision is not comparable to complex climate-chemistry models. For example, the developed tool is not suited to compare the climate effect of flights with similar aircraft of different generations or different travel times in the year, meaning that for an individual flight the real climate effect can strongly deviate from the estimated average. It is also not suited to study certain atmospheric characteristics and their impact on the climate effect or the influence of trajectory optimization. To answer those questions more complex models are needed. The main advantage of *FlightClim* is that it produces reasonable estimates including CO_2 and non-CO_2-effects while being easy to use and requiring very few input data per flight, in fact only origin and destination airport as well as aircraft size.

FlightClim is suited for climate footprint assessments by passengers to compare individual flights and even different travel modes (e.g. aircraft, train, car). Organizations can use it for climate effect monitoring as well as for travel planning. Moreover, the tool can be used for scientific research for quick and coarse quantification of the climate effect of even large flight plans, wherever the restrictions of the developed method are acceptable.

6 Conclusions

This study presents two methods for an easy-to-use estimate of the climate effect per flight considering CO_2 and non-CO_2 effects, of which one is included into the flight climate effect estimator *FlightClim v1.0*. The tool is made available as an Excel application, which is available in the Supplementary Material. The estimation only depends on the origin and destination airports and the aircraft size (seat category for MR or MTOW for SR). It is independent from information about the actual flights like the flown trajectory, real fuel burn or current weather. Thereby the estimation describes an average in terms of time of the year and day as well as aircraft and assumes great circle trajectories. The estimation methods are based on a global dataset of ATR100 climate effects per flight for CO_2, H_2O, NO_x and CiC estimated with AirClim representative for jet aircraft with a capacity of 20 to 600 seats.

Potential use cases for *FlightClim* are advanced analyses on the climate effect of a full year airline, as its effect averages over the year, plausibility checks, or a backup when airlines are unable to provide more detailed data on aircraft and engine used, trajectory and deviations flown, and meteorological conditions on the day of flight. *FlightClim* allows an airline to achieve

an initial estimate of the total climate effects of their whole flight network. Additionally it can be used for the extension of online climate effect estimator tools by non-CO_2 effects or to include a comparison of the climate effect of flights into booking platforms considering non-CO_2-effects. However, when applying the estimator its limitations always have to be considered and the methods must only be used for questions they are able to answer. For example, it is not applicable to any kind of flight route optimisation. Further we note that we have not described route-specific uncertainty estimates of the climate effects. The overall non-CO_2 climate effects have large uncertainties and the route-specific estimates are expected to be equally, or possibly even larger, affected. We recommend the inclusion of per flight uncertainty estimates in *FlightClim* in future studies to expand the scope of the tool.

Compared to the predecessor study by Dahlmann et al. (2023), we here expand the area of application building on a global dataset representative for a worldwide flightplan and a wide range of jet aircraft instead of a spatially focused dataset with Airbus A330-200 flight only. We estimate the absolute ATR100 of all species including CO_2 instead of just the species´ ratio to the ATR100 of CO_2. Moreover, we add a wing span-wise adaption of contrail climate effect to the tool-chain of the regression dataset. To account for the larger scope a clustering is introduced, requiring a smoothing of the estimates at the cluster boundaries. In addition this study does consider two different regression methods and contrasts them. Applying the regression model from Dahlmann et al. (2023) to the dataset of this study for all flights with an Airbus A330-200 aircraft shows, that the MR and SR models even surpass the Dahlmann et al. (2023) formulas in estimating the contrail and total climate effect, but are beaten in terms of NO_x and H_2O climate effect. When looking at the whole dataset of different aircraft the new models outplay the formulas only developed for A330 flights for all species resulting in a MARE of 21.8 % (MR) and 25.9 % (SR) in terms of the ratio of total climate effect to CO_2 climate effect compared to 31.5 % for the formulas from Dahlmann et al. (2023). A comparison in terms of R^2 illustrates this difference even clearer, where the R^2 of 0.27 indicates only a really rough correlation for the Dahlmann et al. (2023) model, wheres MR and SR provide valid estimates (0.70, 0.72). This highlights the advantage of the new models to cover a wide range of civil aircraft. A detailed comparison with Dahlmann et al. (2023) is available in Section S6 of the Supplementary Materials.

The introduced *FlightClim* tool goes beyond alternative methods for simplified climate footprint assessment of single flights, because the regressions of the climate response include the regional dependency of climate effects, instead of using constant factors for approximating non-CO_2-effects. Instead of a constant factor with a MARE of 59 % for the dataset of this study *FlightClim* reaches a MARE of 21 %.

The two utilized methods, MR and SR, differ in effort and capabilities of the methods themselves as well as in quality and quantity of the resulting regression formulas. Even though SR is a more advanced and adaptable method, the estimation quality of the resulting formulas of both approaches is similar. The main advantages of the SR-approach are that it uses the continuous MTOW as aircraft size parameter and is more straightforward and thus less complex. However, the MR-formulas are easier to interpret and yield higher quality results for short and medium range flights. Overall both approaches lead to robust models that enable an easy-to-use climate effect estimation for single flights.

The similar quality of both regression methods indicates, that the resulting estimation quality is not primarily limited by the used regression method, but rather by the complexity of the database and the regression parameters as well as the settings for

the regression analyses and the physical dynamics themselves, hindering a better estimate with a simplified approach based on only OD-pair and aircraft size.. To utilize the whole potential of advanced methods like the symbolic regression those aspects have to be improved first. For example overcoming the limitation of a small number of reference aircraft types included in the dataset could improve the applicability and the overall estimation quality. As another major potential improvement for further studies, the error metric of the regression was identified, as it quantifies the estimation error and serves as the optimization factor during the regression analysis. In this study, error metrics based on the absolute estimation error were used. As the range of values for the climate impact of flights in the dataset is huge due to large differences in aircraft sizes and flight distances, for flights with small climate impacts the relative quality of estimation can drop significantly compared to flights with higher impacts, because of the absolute optimization incentive. Therefore an adjustment in the error metric might be necessary to achieve regressions of a better and more equally distributed estimation quality in further studies and to exploit the whole potential of advanced regression methods.

Code availability. The python code used for the clustering and generation of the MR climate effect functions as well as the Matlab code for the derivation of the SR formulas are provided in Bruder et al. (2025, DOI: https://doi.org/10.5281/zenodo.17184041).

Author contributions. R. N. T. performed the clustering, the Multiple Regressions for the climate effect functions, created figures, and wrote a first version of the manuscript. H. B. performed the symbolic Regressions, adopted the manuscript and the figures and created the Excel tool. F. L. simulated the trajectories and created the emissions inventory. K. D. computed the aviation climate effects using AirClim. M. N. created the regressions for fuel use and NO_x emissions and the Excel tool. S. U. provided the contrail wingspan adaption formulas. All authors helped with discussions, conceptualizing the research and finalizing the paper.

Competing interests. Volker Grewe and Simon Unterstrasser are members of the editorial board of the journal.

Acknowledgements. This work is part of the project „Untersuchung der praktischen Umsetzung der Einbringung von Nicht-CO_2-Treibhausgas-Effekten im Luftverkehr in das EU-ETS einschließlich Clusteranalyse“, funded by the German Environment Agency (Umweltbundesamt – UBA). This work also received funding from CE Delft for regional jets adaptations.

References

Bruder, H., Thor, R. N., Niklaß, M., Dahlmann, K., Eichinger, R., Linke, F., Grewe, V., Unterstrasser, S., and Matthes, S.: Code used in "The DLR CO2-equivalent estimator FlightClim v1.0: an easy-to-use estimation of per flight CO2 and non-CO2 climate effects" (Bruder et al., GMD, 2025), Zenodo, https://doi.org/10.5281/zenodo.17184041, 2025.

Burkhardt, U. and Kärcher, B.: Global radiative forcing from contrail cirrus, Nature Clim. Change, 1, 54–58, https://doi.org/10.1038/nclimate1068, 2011.

Cames, M., Graichen, J., Siemons, A., and Cook, V.: Emission reduction targets for international aviation and shipping, Tech. Rep. IP/A/ENVI/2015-11, Policy Department A for the Committee on Environment, Public Health and Food Safety (ENVI), 2015.

Dahlmann, K., Grewe, V., Frömming, C., and Burkhardt, U.: Can we reliably assess climate mitigation options for air traffic scenarios despite large uncertainties in atmospheric processes?, Transportation Research Part D: Transport and Environment, 46, 40–55, https://doi.org/10.1016/j.trd.2016.03.006, 2016a.

Dahlmann, K., Koch, A., Linke, F., Lührs, B., Grewe, V., Otten, T., Seider, D., Gollnick, V., and Schumann, U.: Climate-Compatible Air Transport System – Climate Impact Mitigation Potential for Actual and Future Aircraft, Aerospace, 3, 38, https://doi.org/10.3390/aerospace3040038, 2016b.

Dahlmann, K., Grewe, V., Matthes, S., and Yamashita, H.: Climate assessment of single flights: Deduction of route specific equivalent CO_2 emissions, International Journal of Sustainable Transportation, 17, 29–40, https://doi.org/10.1080/15568318.2021.1979136, 2023.

Delbecq, S., Fontane, J., Gourdain, N., Planès, T., and Simatos, F.: Sustainable aviation in the context of the Paris Agreement: A review of prospective scenarios and their technological mitigation levers, Progress in Aerospace Sciences, 141, 100 920, https://doi.org/https://doi.org/10.1016/j.paerosci.2023.100920, 2023.

DuBois, D. and Paynter, G. C.: "Fuel Flow Method 2" for Estimating Aircraft Emissions, SAE Transactions, 115, 1–14, https://doi.org/10.2307/44657657, 2006.

EASA: EU FLIGHT EMISSIONS LABEL (FEL) - Draft manual version 0.2, https://www.flightemissions.eu/sites/default/files/media/files/2025-07/FEL_Public_Manual_2025-v0.2.pdf, accessed: 2025-08-21, 2025.

Economics, I. S. .: Air Passenger Market Analysis: November 2023, https://www.iata.org/en/iata-repository/publications/economic-reports/air-passenger-market-analysis---november-2023/, accessed: 2025-06-05, 2024.

EEA: EMEP/EEA air pollutant emission inventory guidebook 2023, https://doi.org/10.2800/795737, 2023.

Faber, J., Greenwood, D., Lee, D., Mann, M., de Leon, P. M., Nelissen, D., Owen, B., Ralph, M., Tilston, J., van Velzen, A., and van de Vreede, G.: Lower NO_x at higher altitudes policies to reduce the climate impact of aviation NO_x emission, Tech. Rep. 08.7536.32, CE Delft, 2008.

Fichter, C.: Climate Impact of Air Traffic Emissions in Dependency of the Emission Location, Ph.D. thesis, Manchester Metropolitan University, Manchester, UK, 2009.

Forster, P. M. d. F., Shine, K. P., and Stuber, N.: It is premature to include non-CO2 effects of aviation in emission trading schemes, Atmospheric Environment, 40, 1117–1121, https://doi.org/10.1016/j.atmosenv.2005.11.005, 2006.

Foundation myclimate: CO2 Flight Calculator, https://co2.myclimate.org/en/flight_calculators/new, accessed: 2025-08-21, 2025.

Ghosh, R., Wicke, K., Kölker, K., Terekhov, I., Linke, F., Niklaß, M., Lührs, B., and Grewe, V.: An Integrated Modelling Approach for Climate Impact Assessments in the Future Air Transportation System–Findings from the WeCare Project, in: 2nd ECATS Conference 2016, 2016.

Google: Travel Impact Module, https://travelimpactmodel.org/, accessed: 2025-08-21, 2025.

Grewe, V. and Stenke, A.: AirClim: an efficient tool for climate evaluation of aircraft technology, Atmospheric Chemistry and Physics, 8, 4621–4639, https://doi.org/10.5194/acp-8-4621-2008, 2008.

Grewe, V., Frömming, C., Matthes, S., Brinkop, S., Ponater, M., Dietmüller, S., Jöckel, P., Garny, H., Tsati, E., Dahlmann, K., Søvde, O. A., Fuglestvedt, J., Berntsen, T. K., Shine, K. P., Irvine, E. A., Champougny, T., and Hullah, P.: Aircraft routing with minimal climate impact: the REACT4C climate cost function modelling approach (V1.0), Geoscientific Model Development, 7, 175–201, https://doi.org/10.5194/gmd-7-175-2014, 2014.

Grewe, V., Dahlmann, K., Flink, J., Frömming, C., Ghosh, R., Gierens, K., Heller, R., Hendricks, J., Jöckel, P., Kaufmann, S., Kölker, K., Linke, F., Luchkova, T., Lührs, B., Van Manen, J., Matthes, S., Minikin, A., Niklaß, M., Plohr, M., Righi, M., Rosanka, S., Schmitt, A., Schumann, U., Terekhov, I., Unterstrasser, S., Vázquez-Navarro, M., Voigt, C., Wicke, K., Yamashita, H., Zahn, A., and Ziereis, H.: Mitigating the climate impact from aviation: Achievements and results of the DLR WeCare project, Aerospace, 4, 34, https://doi.org/10.3390/aerospace4030034, 2017a.

Grewe, V., Matthes, S., Frömming, C., Brinkop, S., Jöckel, P., Gierens, K., Champougny, T., Fuglestvedt, J., Haslerud, A., Irvine, E., and Shine, K.: Feasibility of climate-optimized air traffic routing for trans-Atlantic flights, Environmental Research Letters, 12, 034 003, https://doi.org/10.1088/1748-9326/aa5ba0, 2017b.

Grewe, V., Gangoli Rao, A., Grönstedt, T., Xisto, C., Linke, F., Melkert, J., Middel, J., Ohlenforst, B., Blakey, S., Christie, S., Matthes, S., and Dahlmann, K.: Evaluating the climate impact of aviation emission scenarios towards the Paris agreement including COVID-19 effects, Nature Communications, 12, 3841, https://doi.org/10.1038/s41467-021-24091-y, 2021.

ICAO: Annual Report of the ICAO Council: 2015, https://www.icao.int/annual-report-2015/Documents/Appendix_1_en.pdf, accessed: 2023-02-22, 2015.

ICAO: Annual Report of the ICAO Council: 2021, https://www.icao.int/annual-report-2021/Documents/ARC_2021_Air%20Transport%20Statistics_final_sched.pdf, accessed: 2023-02-22, 2021.

ICAO: Aircraft Engine Emissions Data Bank, Version 29B, http://easa.europa.eu/document-library/icao-aircraft-engine-emissions-databank, accessed: 2024-01-22, 2023.

ICAO: ICAO Carbon Emissions Calculator, https://www.icao.int/environmental-protection/CarbonOffset, accessed: 2025-08-21, 2025.

IEA: Aviation, https://www.iea.org/reports/aviation, accessed: 2023-05-17, 2022.

IPCC: The Supplementary Report to the IPCC Scientific Assessment, in: Climate Change 1992, edited by Houghton, J. T., Callander, B. A., and Varney, S. K., WMO/UNEP, Cambridge University Press, Cambridge, UK, 200 pp., 1992.

IPCC: Aviation and the global atmosphere, in: A Special Report of the Intergovernmental Panel on Climate Change, edited by Penner, J. E., Lister, D., Griggs, D. J., Dokken, D. J., and McFarland, M., Cambridge University Press, 1999.

Kärcher, B.: Formation and radiative forcing of contrail cirrus, Nature Communications, 9, 1824, https://doi.org/10.1038/s41467-018-04068-0, 2018.

Koza, J. R.: Genetic Programming: On the Programming of Computers by Means of Natural Selection, vol. 1 of *A Bradford book*, MIT Press, Cambridge, Mass., 1992.

Larsson, J., Elofsson, A., Sterner, T., and Akerman, J.: International and national climate policies for aviation: a review, . Climate Policy, 19, 787–799, https://doi.org/10.1080/14693062.2018.1562871, 2019.

Lee, D., Fahey, D., Skowron, A., Allen, M., Burkhardt, U., Chen, Q., Doherty, S., Freeman, S., Forster, P., Fuglestvedt, J., Gettelman, A., De León, R., Lim, L., Lund, M., Millar, R., Owen, B., Penner, J., Pitari, G., Prather, M., Sausen, R., and Wilcox, L.:

The contribution of global aviation to anthropogenic climate forcing for 2000 to 2018, Atmospheric Environment, 244, 117 834, https://doi.org/10.1016/j.atmosenv.2020.117834, 2021.

Linke, F.: Environmental Analysis of Operational Air Transportation Concepts, Ph.D. thesis, Hamburg University of Technology, 2016.

Lührs, B., Linke, F., and Gollnick, V.: Erweiterung eines Trajektorienrechners zur Nutzung meteorologischer Daten für die Optimierung von Flugzeugtrajektorien, in: 63. Deutscher Luft- und Raumfahrtkongress 2014 (DLRK), 2014.

Lührs, B., Niklaß, M., Froemming, C., Grewe, V., and Gollnick, V.: Cost-Benefit Assessment of 2D- and 3D Climate and Weather Optimized Trajectories, ATIO, 16, https://doi.org/10.2514/6.2016-3758, 2016.

Lührs, B., Linke, F., Matthes, S., Grewe, V., and Yin, F.: Climate Impact Mitigation Potential of European Air Traffic in a Weather Situation with Strong Contrail Formation, Aerospace, 8, https://doi.org/10.3390/aerospace8020050, 2021.

Märkl, R. S., Voigt, C., Sauer, D., Dischl, R. K., Kaufmann, S., Harlaß, T., Hahn, V., Roiger, A., Weiß-Rehm, C., Burkhardt, U., Schumann, U., Marsing, A., Scheibe, M., Dörnbrack, A., Renard, C., Gauthier, M., Swann, P., Madden, P., Luff, D., Sallinen, R., Schripp, T., and Le Clercq, P.: Powering aircraft with 100 % sustainable aviation fuel reduces ice crystals in contrails, Atmospheric Chemistry and Physics, 24, 3813–3837, https://doi.org/10.5194/acp-24-3813-2024, 2024.

Martin Frias, A., Shapiro, M. L., Engberg, Z., Zopp, R., Soler, M., and Stettler, M. E. J.: Feasibility of contrail avoidance in a commercial flight planning system: an operational analysis, Environ. Res.: Infrastruct. Sustain., 4, 015 013, https://doi.org/10.1088/2634-4505/ad310c, 2024.

Matthes, S., Lim, L., Burkhardt, U., Dahlmann, K., Dietmüller, S., Grewe, V., Haslerud, A. S., Hendricks, J., Owen, B., Pitari, G., Righi, M., and Skowron, A.: Mitigation of non-CO_2 aviation's climate impact by changing cruise altitudes, Aerospace, 8, 36, https://doi.org/10.3390/aerospace8020036, 2021.

Megill, L., Deck, K., and Grewe, V.: Alternative Climate Metrics to the Global Warming Potential Are More Suitable for Assessing Aviation Non-CO2 Effects, Communications Earth & Environment, 5, 249, 2024.

Meinshausen, M., Smith, S. J., Calvin, K., Daniel, J. S., Kainuma, M. L. T., Lamarque, J.-F., Matsumoto, K., Montzka, S. A., Raper, S. C. B., Riahi, K., Thomson, A., Velders, G. J. M., and van Vuuren, D. P. P.: The RCP greenhouse gas concentrations and their extensions from 1765 to 2300, Climatic Change, 109, 213–241, https://doi.org/10.1007/s10584-011-0156-z, 2011.

Niklaß, M., Dahlmann, K., Grewe, V., Maertens, S., Plohr, M., Scheelhaase, J., Schwieger, J., Brodmann, U., Kurzböck, C., Schweizer, N., and von Unger, M.: Integration of Non-CO_2 Effects of Aviation in the EU ETS and under CORSIA, Tech. Rep. (UBA-FB) FB000270/ENG, German Environment Agency, 2019.

Niklaß, M., Grewe, V., Gollnick, V., and Dahlmann, K.: Concept of climate-charged airspaces: a potential policy instrument for internalizing aviation's climate impact of non-CO_2 effects, Climate Policy, 21, 1066, https://doi.org/10.1080/14693062.2021.1950602, 2021.

Niklaß, M., Zengerling, Z., Mendiguchia Meuser, M., Eichinger, R., Ehlers, T., Lau, A., Yin, F., Stefanidi, A., and Grewe, V.: Impact of Non-CO_2 Pricing on Routing and Ticket Fares in Aviation: Strategies to Address Uncertainties in Climate Policies, Pre-Print, https://zenodo.org/records/15438171, 2025.

Pedregosa, F., Varoquaux, G., Gramfort, A., Michel, V., Thirion, B., Grisel, O., Blondel, M., Prettenhofer, P., Weiss, R., Dubourg, V., Vanderplas, J., Passos, A., Cournapeau, D., Brucher, M., Perrot, M., and Duchesnay, E.: Scikit-learn: Machine Learning in Python, Journal of Machine Learning Research, 12, 2825–2830, 2011.

Prather, M. J., Gettelman, A., and Penner, J. E.: Trade-offs in aviation impacts on climate favour non-CO_2 mitigation, Nature, 643, 988–993, https://doi.org/10.1038/s41586-025-09198-2, 2025.

Quante, G., Enderle, B., Laybourn, P., Holm, P. W., Andersen, L. W., Voigt, C., and Kaltschmitt, M.: Segregated supply of Sustainable Aviation Fuel to reduce contrail energy forcing – demonstration and potentials, Journal of the Air Transport Research Society, 4, 100 049, https://doi.org/https://doi.org/10.1016/j.jatrs.2024.100049, 2025.

Sausen, R., Hofer, S., Gierens, K., Bugliaro, L., Ehrmanntraut, R., Sitova, I., Walczak, K., Burridge-Diesing, A., Bowman, M., and Miller, N.: Can we successfully avoid persistent contrails by small altitude adjustments of flights in the real world?, Meteorologische Zeitschrift, 33, 83–98, https://doi.org/10.1127/metz/2023/1157, 2024.

Scheelhaase, J. D., Dahlmann, K., Jung, M., Keimel, H., Nieße, H., Sausen, R., Schaefer, M., and Wolters, F.: How to best address aviation's full climate impact from an economic policy point of view? – Main results from AviClim research project, Transportation Research Part D: Transport and Environment, 45, 112–125, https://doi.org/10.1016/j.trd.2015.09.002, 2016.

Searson, D. P.: GPTIPS 2: An Open-Source Software Platform for Symbolic Data Mining, in: Handbook of Genetic Programming Applications, edited by Gandomi, A. H., Alavi, A. H., and Ryan, C., pp. 551–573, Springer International Publishing, Cham, https://doi.org/10.1007/978-3-319-20883-1_22, 2015.

Silberhorn, D., Dahlmann, K., Görtz, A., Linke, F., Zanger, J., Rauch, B., Methling, T., Janzer, C., and Hartmann, J.: Climate Impact Reduction Potentials of Synthetic Kerosene and Green Hydrogen Powered Mid-Range Aircraft Concepts., Appl. Sci., 12, https://doi.org/10.3390/app12125950, 2022.

Stenke, A., Dameris, M., Grewe, V., and Garny, H.: Implications of Lagrangian transport for simulations with a coupled chemistry-climate model, Atmospheric Chemistry and Physics, 9, https://doi.org/10.5194/acp-9-5489-2009, 2009.

Teoh, R., Schumann, U., Majumdar, A., and Stettler, M.: Mitigating the Climate Forcing of Aircraft Contrails by Small-Scale Diversions and Technology Adoption, Environ. Sci. Technol., 54, https://doi.org/10.1021/acs.est.9b05608, 2020.

Teoh, R., Schumann, U., Voigt, C., Schripp, T., Shapiro, M., Engberg, Z., Molloy, J., Koudis, G., and Stettler, M.: Targeted Use of Sustainable Aviation Fuel to Maximize Climate Benefits, Environ. Sci. Technol., 56, https://doi.org/10.1021/acs.est.2c05781, 2022.

Unterstrasser, S. and Görsch, N.: Aircraft-type dependency of contrail evolution, J. Geophys. Res. Atmos., 119, 14 015–14 027, https://doi.org/10.1002/2014JD022642, 2014.

Yin, F., Grewe, V., Castino, F., Rao, P., Matthes, S., Dahlmann, K., Dietmüller, S., Frömming, C., Yamashita, H., Peter, P., Klingaman, E., Shine, K. P., Lührs, B., and Linke, F.: Predicting the climate impact of aviation for en-route emissions: the algorithmic climate change function submodel ACCF 1.0 of EMAC 2.53, Geoscientific Model Development, 16, 3313–3334, https://doi.org/10.5194/gmd-16-3313-2023, 2023.